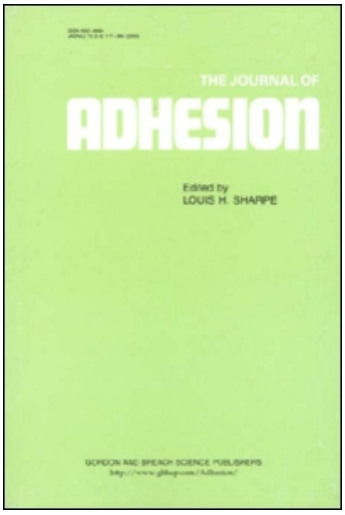

The Journal of Adhesion
Publication details, including instructions for authors and subscription information:
http://www.informaworld.com/smpp/title~content=t713453635

Incorporating Environmental Degradation in Closed Form Adhesive Joint Stress Analyses

A. D. Crocombe[a]
[a] Faculty of Engineering and Physical Sciences, University of Surrey, UK

To cite this Article Crocombe, A. D.(2008) 'Incorporating Environmental Degradation in Closed Form Adhesive Joint Stress Analyses', The Journal of Adhesion, 84: 3, 212 — 230
To link to this Article: DOI: 10.1080/00218460801954268
URL: http://dx.doi.org/10.1080/00218460801954268

The Journal of Adhesion, 84:212–230, 2008

ISSN: 0021-8464 print/1545-5823 online
DOI: 10.1080/00218460801954268

Taylor & Francis
Taylor & Francis Group

Incorporating Environmental Degradation in Closed Form Adhesive Joint Stress Analyses

A. D. Crocombe
Faculty of Engineering and Physical Sciences, University of Surrey, UK

A review of the literature reveals that although the effects of environmental degradation have been incorporated into some recent finite element stress analyses of adhesive joints, closed form solutions have not yet been developed. Due to its ease of use, such a closed form approach would be very useful for screening analyses of potential joint configurations. Two different closed form approaches have been developed. Both use simple, yet demonstrably reasonable, assumptions about the affect of moisture on the mechanical properties of the adhesive and both use a Fickian diffusion model to determine moisture distribution in the joint. The simplest approach is based on limit state assumptions and results in a simple non-dimensionalised equation relating residual strength to the time of exposure. The equation is in the form of an infinite series and is also presented as a design chart for even easier access. The second approach is the adaptation of a generalised non-linear adhesive sandwich analysis. The advantage of this is that it is applicable to a wide range of bonded joints and not just the single lap joint in the closed form solution. Further, it is not limited by limit state assumptions and gives the adhesive peel and shear stress distribution for any loading condition and exposure time. Both approaches were illustrated by the application to a typical single lap joint, exposed at 85% RH for 230 days.

Keywords: Bonded joint design tool; Closed form bonded joint analysis; Durability modelling; General joint analysis; Global yielding; Limit state; Material degradation

1. INTRODUCTION

One of the major challenges facing the adhesive technologist is ensuring joint integrity in the presence of a wet environment.

Received 10 September 2007; in Final Form 16 November 2007
One of a Collection of papers honoring John Watts, the recipient in Febraury 2008 of *The Adhesion Society Award for Excellence in Adhesion Science, Sponsored by 3M*.
Address correspondence to A. D. Crocombe, Faculty of Engineering and Physical Sciences (H5), University of Surrey, Guildford GU2 7XH, UK. E-mail: a.crocombe@surrey.ac.uk

Moisture penetrates the joint and can degrade both the cohesive properties of the adhesive and the interface between the adhesive and substrate. Watts and co-workers [1–3] and others have undertaken excellent work investigating the nature of this degradation at a molecular level using surface science techniques. Clearly it is important to be able to use this and other information when designing adhesively bonded structures to ensure their fitness for purpose. One way of validating a bonded joint design is through long term exposure and testing. This is being undertaken [4,5] but does carry significant time penalties. In an attempt to overcome this problem researchers have used more aggressive environments to accelerate the degradation [6]. However, there is always the concern that a degradation mechanism will be induced in this accelerated testing that does not occur in service conditions.

An alternative approach is to develop predictive modelling techniques that simulate the response of a bonded structure to service conditions. Recently, significant advances have been made in this area [7,8] with coupled mechanical-diffusion finite element analyses that can incorporate hygro-thermal residual, as well as mechanical, stresses together with progressive damage modelling controlled by environmental dependent damage parameters. Such analyses are extremely computationally intensive and require considerable expertise to implement. In order to allow for a more rapid, preliminary screening of candidate bonded joints it would be useful to have an analysis tool that is more readily accessible. Analyses where the governing equations have been formulated specifically for adhesive joints can provide this sort of ease of solution and accessibility. Such analyses are commonly termed "closed form" analyses in comparison with the more open or generalised nature of finite element analyses.

There is a long history of closed form adhesive joint analyses commonly believed to start with the shear lag approach outlined by Volkersen [9]. A detailed account of these analyses can be found elsewhere [10] and only a brief summary is given here. Volkersen's analysis neglects peel stresses and, hence, is more applicable to a double lap joint. A characteristic of this and all subsequent analyses is the peaking of the adhesive stresses at the overlap ends where the load transfer from one substrate through the adhesive to the other substrate occurs. Goland and Reissner [11] included substrate bending in their analysis of the single lap joint and this enabled expressions to be developed for adhesive peel as well as shear stresses. Also, an expression was developed that gave the substrate bending moment and consequently the shear force in terms of the applied axial load.

Following this, Volkersen [12] extended their original analysis to include the adhesive peel stresses. Unlike the outer substrates the centre substrate experienced no bending.

Renton and Vinson [13] made the next significant contribution to the analysis of single lap joints, including the effect of shearing in orthotropic substrates. The maximum peel and shear stresses are somewhat lower than those found by Goland and Reissner [11]. The adhesive shear and peel stress were still assumed constant across the thickness of the adhesive. Ojalvo and Eidinoff [14] incorporated a linear variation of shear strain across the adhesive thickness but neglected substrate shearing. This allowed the adhesive shear stress to become zero at the free surface at the overlap ends. Delale *et al.* [15] included adhesive longitudinal stress, in addition to the shear and peel stresses; however, these adhesive stresses were assumed constant across the adhesive thickness. Yang and Pang [16] used a Fourier series approach to model unbalanced joints with three adhesive stress components included. A different way of modelling substrate shear was introduced by Tsai *et al.* [17], but only the adhesive shear stress was included. Sawa and Suga. [18] modelled an unbalanced single lap joint by considering the two substrates and the adhesive layer as three separate strips, subjected to common but unknown traction along the interfaces and appropriate tractions on the other faces.

A number of authors including Allman [19] and Adams and Mallick [20] have adopted a different approach to obtain a global stress analysis of adhesive joints, applying the variational principle of complementary energy. There is generally good correlation between these analyses and the more conventional closed form solutions.

To a certain extent these refinements in the distribution of stress across the adhesive thickness are of more theoretical than practical interest. The reason for this is that an exact solution for the linear elastic stresses in an adhesive joint [21] show that the stresses are infinite due to the bi-material singularities that occur at the overlap ends. In the context of bonded joint design there are various ways of dealing with this singularity that include a) defining the singularity strength and intensity (much like conventional fracture mechanics) and b) processing the stress or strain field over a finite zone surrounding the singular point [22]. One very common approach is to average the adhesive stresses across the adhesive layer and this, in essence, is what the early closed form analyses do.

All the analyses discussed above assume linear behaviour of the adhesive and substrate. Many modern adhesive systems exhibit

significant non-linearity in their stress strain behaviour and, hence, analyses based on linear material behaviour may be of limited use for strength assessment. To overcome this Hart-Smith [23,24] extended double and single lap joint analyses, modelling the adhesive as an elasto-plastic material. The analyses were simplified by uncoupling the shear and peel stresses, assuming elasto-plastic behaviour for the former and elastic for the latter. By assuming that joint failure occurs at a critical level of plastic strain, Hart-Smith developed design charts for predicted joint strength.

The solutions above have been derived for specific joint configurations (*i.e.* single and double lap joints) and, thus, are of limited use for application to a wider range of joint configurations. Bigwood and Crocombe [25,26] generalised the solution of Goland and Reissner [11] for an arbitrarily end loaded overlap, thus widening its range of applicability considerably, as illustrated in Fig. 1. They incorporated a full non-linear representation of the adhesive layer where both the peel and shear stresses contribute to adhesive yield. Good correlation was found between their analyses and non-linear FE solutions. This

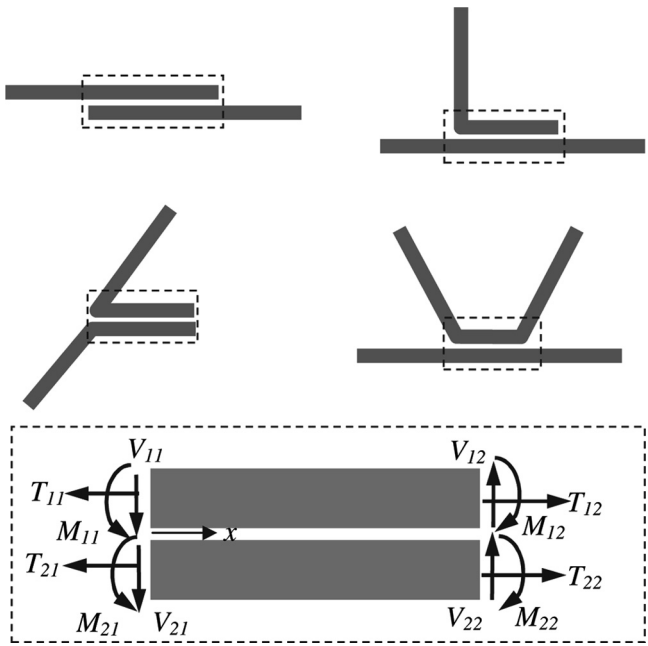

FIGURE 1 A selection of potential joint configurations all of which contain an end loaded overlap.

was extended further [27] to include plastic deformation in the substrates as well as the adhesive. It should be pointed out that the substrate moment, shear, and axial loads are required at the overlap ends. These end loads may be found directly or, for more complex configurations, from an analysis of the structure containing the joint. In these structural analyses it is not necessary to model the joint in detail.

Weitsman [28] and others (*e.g.* [20]) have included the swelling effect of hygrothermal strains in lap joint analysis as an initial strain but do not model the degradation of material properties that is induced by the moisture. It can be seen that the basic closed form approach has been developed to accommodate non-linear material behaviour of arbitrary joint configurations. However, these analyses cannot currently accommodate any form of material environmental degradation and this is the purpose of the work discussed in this paper. Two separate approaches have been outlined. In the following section an estimate for the reduced strength of a joint exposed to environmental degradation has been derived based on a limit state assumption. This results in a simple equation and a chart for the upper bound of the failure load of a degraded single or double lap joint. This is followed by a section that outlines the extension of the non-linear arbitrarily end loaded overlap closed form analysis of Bigwood and Crocombe [26] to accommodate moisture dependent material parameters. This second approach is applicable to a wide range of adhesive joints, as illustrated in Fig. 1.

2. LIMIT STATE SOLUTION FOR ENVIRONMENTALLY DEGRADED ADHESIVE SINGLE LAP JOINTS

A limit state solution gives an upper bound to joint strength, the failure load being found by assuming that all the adhesive reaches its maximum load carrying capacity before joint failure occurs. Crocombe [29] termed this "global yielding" and showed that it was applicable to a wide range of lap joints. Such joints should be able to reach yield over most of the adhesive layer before local failure of the adhesive at the overlap ends occurs. This obviously depends on the ductility of the adhesive and the overlap length. Global yielding can be applied to most conventional single and double lap joints constructed with modern adhesives, but will be less applicable as the overlap length increases.

In this solution a limit state load is found for a 2-D representation of a joint following exposure to a known environment for a known period

of time. It has been assumed that the transport of the moisture into the joint is governed by Fickian diffusion and, thus, from standard texts such as Crank [30] it can be shown that the moisture concentration (c) at a certain distance from the overlap end (x) within an initially dry ($c = 0$) joint of overlap length (L) at a time (t) is given by Eq. (1), where c_o is the saturation moisture uptake of the adhesive and D is the diffusion coefficient:

$$c(x,t) = c_o - \sum_0^\infty \frac{4c_o}{(2j+1)\pi} \sin\left[\frac{(2j+1)\pi x}{L}\right] e^{\frac{-(2j+1)^2 D\pi^2 t}{L^2}}. \quad (1)$$

This is illustrated schematically in Fig. 2.

The constitutive response of adhesives is known to be a function of moisture content. Both the modulus and ultimate strength reduce with increasing moisture content. Data measured within the author's group [31–33] for four structural adhesives are shown in Table 1. It can be seen that the degree of degradation varies and that there appears to be a correlation with the maximum water uptake. Data for one of these adhesive systems (B) are shown in more detail in Fig. 3 and this has formed the basis for modelling later in this paper. It can be seen that the reduction in both modulus and flow stress with moisture is essentially linear and the analysis developed in this section makes use of this observation.

From basic equilibrium the limit state load ($P_{\max}$) carried by a single lap joint can be obtained by integrating the maximum adhesive shear

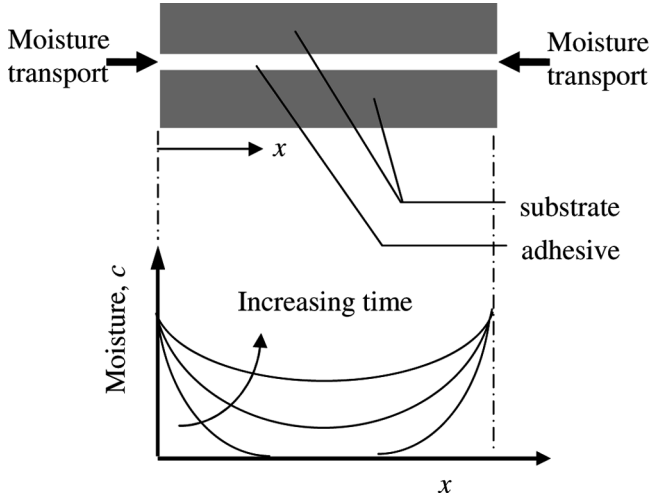

FIGURE 2 Moisture distribution within the adhesive joint.

TABLE 1 Moisture Degraded Modulus and Strength Values for Four Different Structural Adhesives

Adhesive	Saturated moisture uptake (%)	Dry modulus (MPa)	Saturated modulus (MPa)	Dry strength (MPa)	Saturated strength (MPa)
A	9.0	2000	340	32	13
B	7.6	2800	1800	65	30
C	3.9	2900	2500	53	48
D	2.0	2000	1500	45	32

stress (τ_{max}) along L. As τ_{max} reduces with increasing moisture content the τ_{max} attainable by the adhesive is higher in the (drier) centre of the overlap than the (wetter) outer region. This is illustrated schematically in Fig. 4 and Eq. (2):

$$P_{max} = \int_0^L \tau_{max}(c/c_o)dx. \tag{2}$$

By assuming that τ_{max} varies linearly with c from a value of τ_{dry} when $c = 0$, to a value of τ_{wet} when $c = c_o$, the maximum shear stress can be

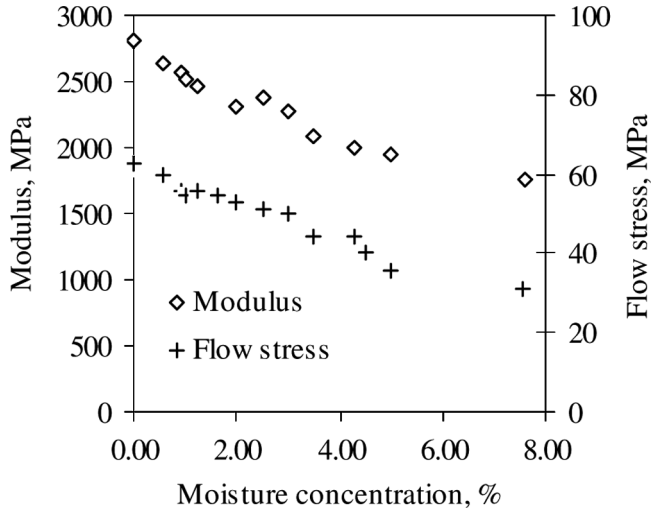

FIGURE 3 Variation of modulus and ultimate strength of a toughened epoxy with moisture.

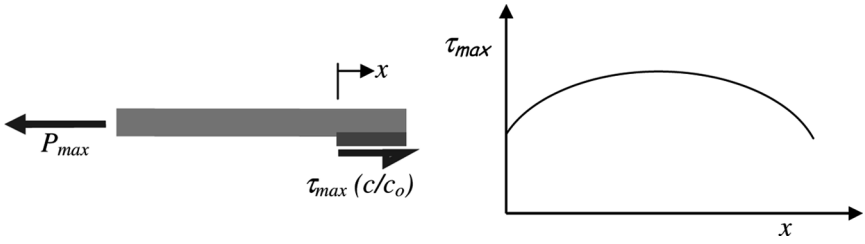

FIGURE 4 Schematic illustration of limit state load evaluation.

expressed as

$$\frac{\tau_{\max}}{\tau_{\text{dry}}} = 1 - \frac{c}{c_o}\left(1 - \frac{\tau_{\text{wet}}}{\tau_{\text{dry}}}\right). \tag{3}$$

Substituting Eq. (3) into (2) and manipulating gives:

$$P_{\max} = \tau_{\text{dry}}\left(L - F_\tau \int_0^L \frac{c}{c_o} dx\right), \tag{4}$$

where $F_\tau = 1 - (\tau_{\text{wet}}/\tau_{\text{dry}})$. The parameter F_τ represents the degree of degradation that the adhesive experiences on exposure to moisture. When $F_\tau = 0$ there is no degradation in the adhesive on saturation whilst $F_\tau = 1$ indicates that the adhesive loses all its strength on exposure to moisture. For the adhesives shown in Table 1, F_τ varies between 0.53 and 0.91.

Substituting Eq. (1) into (4) and manipulating gives:

$$P_{\max} = \tau_{\text{dry}}\left(L(1 - F_\tau) + F_\tau \sum_0^\infty \frac{4}{(2j+1)\pi} e^{-(2j+1)^2\left(D\pi^2 t/L^2\right)} \times \int_0^L \sin(2j+1)\frac{\pi x}{L} dx\right). \tag{5}$$

Evaluating the integral in Eq. (5) and simplifying further finally gives:

$$\frac{P_{\max}}{\tau_{\text{dry}} L} = \left[1 - F_\tau\left(1 - \frac{8}{\pi^2}\sum_0^\infty \frac{1}{(2j+1)^2} e^{-(2j+1)^2\left(D\pi^2 t/L^2\right)}\right)\right]. \tag{6}$$

This equation enables the limit state load to be determined for any adhesive system characterised by its dry and saturated ultimate

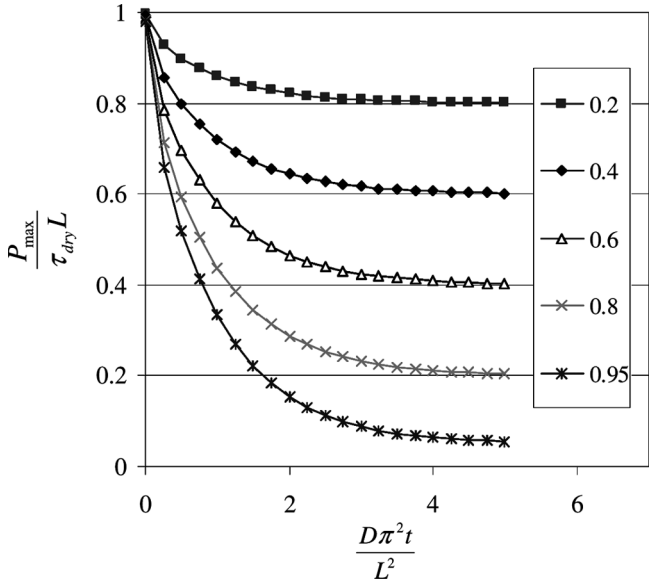

FIGURE 5 Showing the variation of the normalised limit state load with non-dimensionalised time of exposure for a range of F_τ values.

stresses, the diffusion coefficient, the time of exposure, and the overlap length.

To facilitate the application of this limit state solution, Eq. (6) is presented graphically for a number of F_τ values in Fig. 5. This enables the limit state load to be readily assessed without evaluation of Eq. (6). Further, some important trends can be noted. As expected, the curves become asymptotic to $\tau_{\text{wet}}/\tau_{\text{dry}}$ $(= 1 - F_\tau)$ at long exposure times. Under these conditions the entire overlap is saturated and is, thus, uniformly, fully degraded. At short exposure times the limit state load approaches the fully dry limit state load. At intermediate exposure times the limit state load reduces gradually from the fully dry value to the fully degradaded value.

3. DEVELOPMENT OF THE GENERALISED ADHESIVE SANDWICH (GAS) ANALYSIS TO INCORPORATE ENVIRONMENTAL DEGRADATION

3.1. Derivation and Solution Procedure

The original non-linear GAS analysis, as presented by Bigwood and Crocombe [26], required the solution of the following six non-linear

differential equations:

$$\begin{aligned}
\frac{dT_1}{dx} &= \frac{E_s\gamma_{xy}}{2(1+\nu_p)} \\
\frac{dV_1}{dx} &= \frac{E_s\varepsilon_y}{(1+\nu_p^2)} \\
\frac{dM_1}{dx} &= V_1 - \frac{(h_1+t_a)E_s\gamma_{xy}}{4(1+\nu_p)} \\
\frac{d\varepsilon_y}{dx} &= \kappa \\
\frac{d\kappa}{dx} &= f_1(M_1, T_1, x) \\
\frac{d\gamma_{xy}}{dx} &= f_2(M_1, T_1, x).
\end{aligned} \tag{7}$$

Further details are given in the original paper [26]. In these equations T_1, V_1, and M_1 are the tension, shear, and moment in the upper substrate at a distance x from the overlap end (Fig. 1); h_1 and t_a represent the thickness of the upper substrate and the adhesive layer, respectively. The parameters γ_{xy} and ε_y represent the shear and peel strains in the adhesive corresponding to the adhesive shear and peel stresses, τ_{xy} and σ_y, respectively and κ is simply a dummy variable. Adhesive non-linearity is modelled using a deformation theory of plasticity that links the total stress to the total strain using the secant modulus (E_s) and a plastic Poisson's ratio (ν_p). The secant modulus is defined in terms of the von Mises equivalent adhesive stress (σ_{eq}) and strain (ε_{eq}) as illustrated in Fig. 6 and the plastic Poisson's ratio is defined in Eq. (8), where E and ν are the elastic modulus and Poisson's ratio, respectively:

$$\nu_p = \frac{1}{2}\left[1 - \frac{E_s}{E}(1-2\nu)\right]. \tag{8}$$

Normally, only the adhesive strains (and associated stresses) are required but the upper substrate loads are obtained from the solution and these can be used to find upper substrate stresses and also from equilibrium, lower substrate loads and stresses if required. These equations are solved using a finite difference boundary value procedure. A direct method rather than a shooting method has been used as the full set of boundary conditions at $x = 0$ are not known and the shooting method was found to have convergence problems. The boundary conditions for this problem are the upper substrate tension, shear, and moment at each end of the overlap.

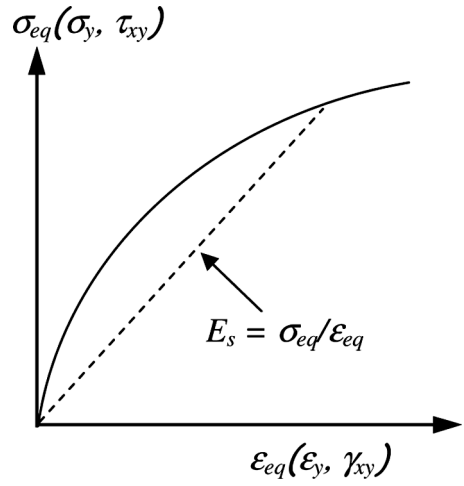

FIGURE 6 Non-linear adhesive stress-strain curve.

The original solution uses a single hyperbolic tangent model to define the generic stress-strain response of the adhesive

$$\sigma_{eq} = A \tan \mathrm{h}\left[\frac{E\varepsilon_{eq}}{A}\right]. \tag{9}$$

All the parameters have been defined above apart from A, which is the ultimate adhesive equivalent stress.

To extend this analysis to include degradation due to moisture it is necessary to replace the single adhesive material model with an infinitely varying material model which is moisture dependent. The solution is then carried out in two steps. The initial step determines the moisture distribution in the adhesive, by the application of Eq. (1). The diffusion coefficient and the saturation moisture uptake are commonly found from gravimetric tests. There is also a considerable amount of published data available for different adhesives. The second step is the stress analysis and here the actual material curve being used at any given point in the adhesive depends upon the moisture and thus the position in the overlap. This is illustrated schematically in Fig. 7, which shows the lowest (most degraded) stress strain curve occurring at the overlap ends where the adhesive is wettest and the highest (least degraded) curve occurring at the centre of the overlap where the adhesive is driest.

Such a moisture dependent material model can be implemented by making the parameters A and E in Eq. (9) moisture dependent.

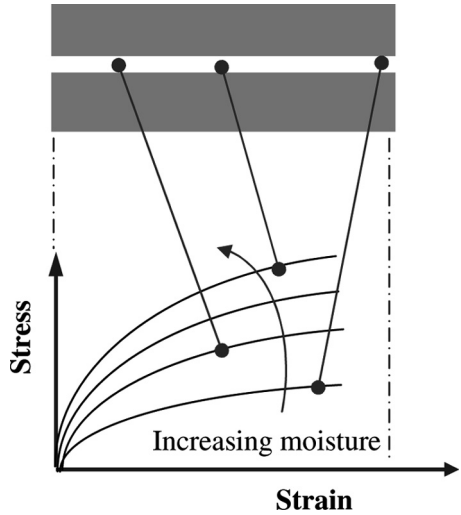

FIGURE 7 Schematic illustration of the moisture dependent adhesive stress strain response.

Typical variation of modulus and ultimate stress with moisture has already been shown in Fig. 3, where it was noticed that both appeared to decrease linearly with increasing moisture content. Thus, the model has been extended by rewriting Eq. (9) as

$$\sigma_{eq} = A_c \tan \mathrm{h}\left[\frac{E_c \varepsilon_{eq}}{A}\right], \tag{10}$$

defining A_c and E_c as:

$$\frac{A_c}{A_{\mathrm{dry}}} = 1 - \frac{c}{c_o}\left(1 - \frac{A_{\mathrm{wet}}}{A_{\mathrm{dry}}}\right) \quad \text{and} \tag{11}$$

$$\frac{E_c}{E_{\mathrm{dry}}} = 1 - \frac{c}{c_o}\left(1 - \frac{E_{\mathrm{wet}}}{E_{\mathrm{dry}}}\right), \tag{12}$$

where subscripts dry and wet refer to the properties at fully dry and fully saturated conditions, respectively, and c and c_0 refer to moisture levels as discussed in Eq (1).

The solution procedure is summarised in the flow chart shown in Fig. 8. In addition to geometry, loads, and substrate material, also required are the dry and wet E and A values, D, and t, all for the environment under consideration.

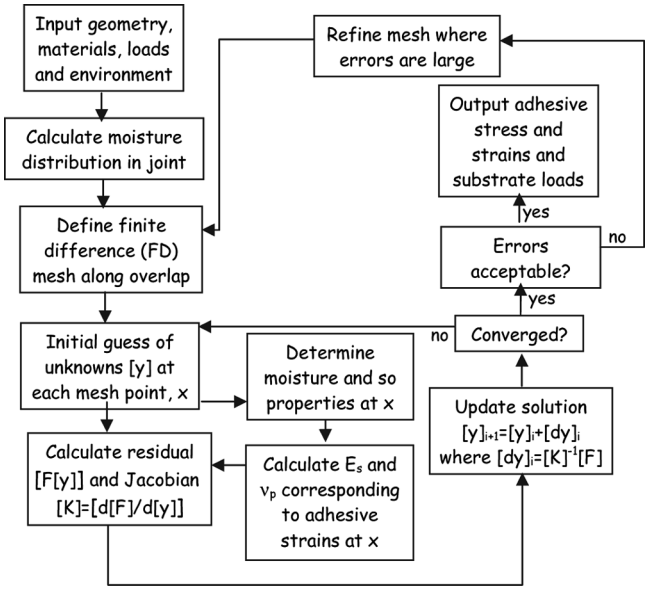

FIGURE 8 Flow chart of the modified GAS solution procedure.

The moisture distribution is calculated analytically using Eq. (1) at a number of points along the adhesive layer. Values of the moisture at positions between these points are found using interpolation. It has been found that only a few terms of the infinite series in Eq. (1) are required to obtain convergence.

An initial finite difference (FD) mesh having $n-1$ equally spaced internal points (and hence n regions) is defined for the solution of the six first order non-linear differential equations presented in Eq. (7). This mesh may be refined (discussed later) if convergence of the non-linear solution process cannot be achieved on this initial mesh. To start the solution, an initial guess for values of all six of the unknowns at all $n+1$ mesh points are required. Linear interpolation can be used for the substrate loads (T_1, V_1, and M_1) as boundary values of these are given at each end of the overlap. It has been found that assuming a value of zero for the other three variables (ε_y, κ, and γ_{xy}) at all points provides an acceptable starting point for the solution.

Each of the six differential equations are written as first order difference equations over each of the n regions. This provides $6n$ equations in the $6(n+1)$ unknowns. The remaining six equations come from the six boundary condition values (the three substrate

loads at each end of the joint). The equations can be expressed in matrix form

$$[\mathrm{K}][\mathrm{y}] - [\mathrm{R}] = [\mathrm{F}] = 0, \tag{13}$$

where $[K]$ is the $6(n+1)$ square matrix of coefficients of the unknowns stored in the $6(n+1)$ column vector $[y]$. The $6(n+1)$ column vector $[R]$ contains the RHS (right hand side) of each of the equations. The $6(n+1)$ column matrix $[F]$ is known as the residual and should be zero when the unknowns (held in $[y]$) take their correct values.

In a linear problem, Eq. (13) can be solved directly to give the unknowns. However, in a non-linear problem such as this, the equations must be solved iteratively. Here a Newton-Raphson approach was adopted. This involved finding the residual and the Jacobian of the residual and using the two to find an improved solution. Both the residual and the Jacobian require E_s and ν_p. Finding these values involves the use of the moisture dependent hyperbolic tangent model evaluated at the appropriate moisture level. The terms E_s and ν_p are coupled and, hence, at each material point an iterative loop is used to find converged values corresponding to the adhesive strains at that point (ε_y and γ_{xy}).

Convergence for such non-linear problems can be difficult and various techniques have been incorporated to enhance the convergence. It is not appropriate to go into detail here but just to indicate that these techniques include ramping in the non-linearity (by incrementing the load) and refining the FD mesh where large errors are identified. The errors are assessed using higher order terms in the FD expansion.

3.2. Validating Analyses

To validate the implementation and illustrate the effectiveness of this solution procedure a set of stress analyses have been undertaken on a typical single lap joint. It should be emphasised that unlike the limit state solution outlined in the previous section this analysis is applicable to any joint geometry that contains an end-loaded substrate-adhesive sandwich.

3.2.1. Configurations Analysed

The single lap joint analysed had 1 mm aluminium substrates, 0.25 mm adhesive layer, and 12.5 mm overlap and was subjected to an axial load of 400 N/mm. This joint configuration is shown in Fig. (9a) and the corresponding end-loaded overlap region is shown in Fig. (9b). The Goland and Reissner [11] bending moment factor

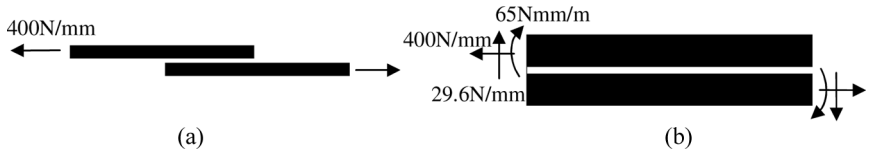

FIGURE 9 Single lap joint configuration and end load conditions.

was used to calculate the corresponding shear and moment loads on the overlap ends.

Three different conditions have been assumed: dry linear material, dry non-linear material, and non-linear material exposed in 85%RH for 230 days. The diffusion coefficient and dry and saturated adhesive modulus (E) and flow stress (A) values are given in Table 1. The data used are representative of typical structural epoxy adhesives. The moisture distribution in the joint after 230 days at 85% RH is shown in Fig. 10. It can be seen that even after such a relatively long exposure period the centre of the joint is reasonably dry. In practice, diffusion would also occur in the adhesive in the out of plane direction. However, as a typical single lap joint width is 25 mm (twice the overlap length), the moisture distribution is dominated by diffusion in the plane.

For clarity the stress strain curves obtained using the material parameters in Table 1 are shown in Fig. 11. Again, it should be emphasized that these are representative properties. It can be seen that both the modulus and the ultimate stress are strongly dependent on the level of moisture in the adhesive. The lowering of the modulus would tend to reduce and spread the adhesive stress and strain state whilst the lowering of the ultimate stress will reduce the load carrying capacity of the joint.

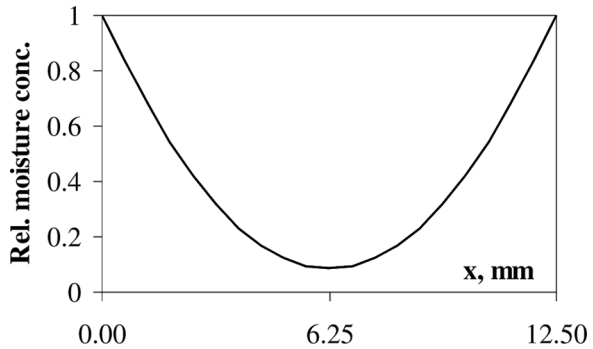

FIGURE 10 Moisture distribution along the overlap after exposure in 85% RH after 230 days.

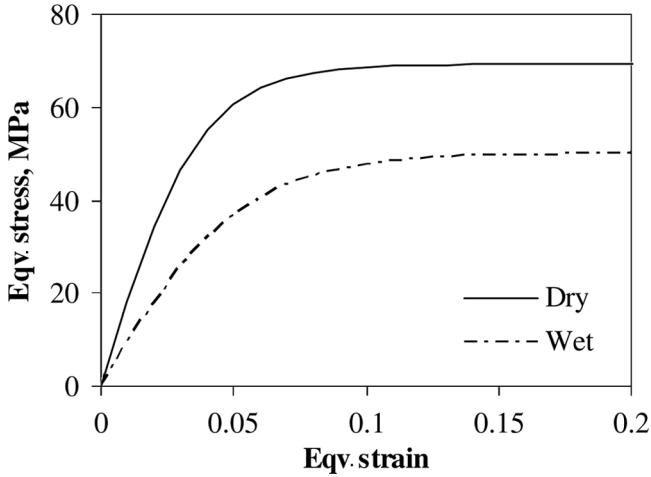

FIGURE 11 Dry and saturated bulk adhesive tensile stress strain curves.

3.2.2. Results and Discussion

The resulting shear stress and shear strain distributions are shown in Fig. 12(a) and (b), respectively. The strains from the analysis with linear material behaviour are the lowest, because in the other analyses the adhesive becomes more flexible and, hence, for a given load the deflection and, thus, the strains will increase. The stress distribution for this linear analysis matches the shape of the strain distribution, which is to be expected from a linear analysis as the modulus is constant.

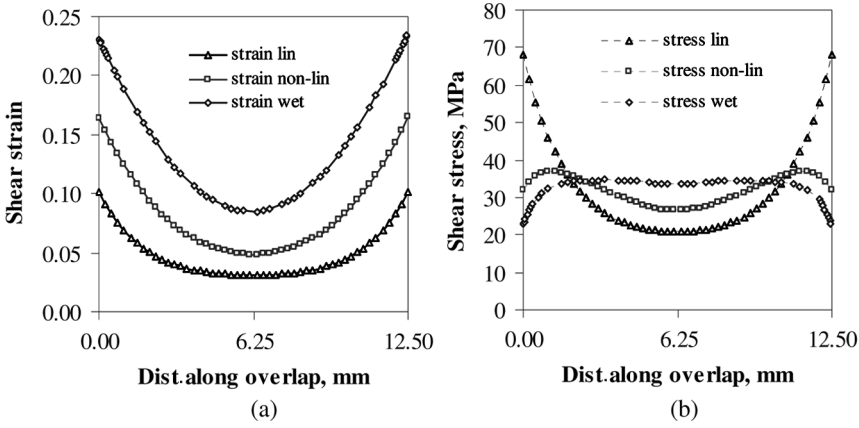

FIGURE 12 Comparison of stress and strain distributions.

Including adhesive plasticity (non-linear) results in higher strains. The strain distribution also becomes more peaky, because yielding spreads in from both ends of the overlap, making the edges relatively more compliant than the center, resulting in a more rapid increase of strains in these outer regions. Consideration of the shear stresses show the yielding that occurs when non-linearity is included. It would appear that, for the level of load considered, the adhesive has yielded over the first few mm at each end of the overlap. Yielding occurs as a result of the shear and peel stresses, which combine to give an equivalent stress. The reason that the shear stresses dip down towards the ends is because in these regions the adhesive peel stress (not shown here) rises quite sharply and the combined equivalent stress cannot exceed the dry ultimate stress of 69.3 MPa.

Strains from the full moisture dependent (wet) analysis are even higher. This is because, in addition to dry yielding, the moisture also reduces the linear modulus and the ultimate stress even further, increasing the flexibility of the adhesive further. The stresses show an interesting trend. The dips at the overlap ends are not only caused by the sharply rising peel stresses contributing to the combined equivalent stresses. The moisture in this end region also reduces the ultimate stress that can be carried. Unlike the dry non-linear stresses the stresses do not dip towards the centre of the joint, even though the shear strains do. This is because of the moisture profile, shown in Fig. 10. The adhesive becomes drier as the centre of the overlap is approached. Thus, at the centre the modulus and ultimate stress are higher and, hence, the adhesive can transmit more stresses even at reduced levels of strain. This higher stress occurring at the centre of the joint is a feature that has been noted elsewhere [34].

An indication of how close the wet analysis was to limit state conditions can be found by using Fig. 5 to evaluate the limit state load. With $D = 2.42 \times 10^{-13}\,\mathrm{m^2/s}$, $t = 230$ days, and $l = 12.5\,\mathrm{mm}$ the abscissa of the graph can be evaluated to be 0.304. Referring to Fig. 5, it can be seen that although this is a relatively low abscissa value a reasonable degree of degradation has occurred. This is entirely consistent with the moisture profile shown in Fig. 10. Table 1 shows that the wet to dry ultimate stress ratio (τ_w/τ_d) is 0.72, which corresponds to an F_τ value of 0.28. The ordinate corresponding to the intersection of this curve and the abscissa value of 0.304 is 0.89. Assuming von Mises yielding, the dry shear strength corresponding to an ultimate stress of 69.3 MPa is 40 MPa. From this and the overlap length the limit state load can be evaluated to be 445 N/mm. As expected, this is a little higher than the load applied in the analysis, which was 400 N/mm. This implies that the wet

analysis results shown in Fig. 12 are reasonably close to the limit state condition.

4. CONCLUSIONS

A brief review of existing closed form adhesive joint analyses has revealed many developments on the original analyses of Goland and Reissner. However, many of these cannot incorporate non-linear material behaviour because of the complexity of their formulations.

Environmental degradation has only been incorporated in stress analyses of joints using complex finite element solutions. No record has been found of any closed form analysis that has been developed to incorporate the degrading effects of moisture on the adhesive material properties.

In this paper two approaches have been outlined for incorporating moisture degradation into closed form solutions. The first is a limit state approach that will be more applicable for shorter overlap or ductile adhesives. Non-dimensionalised results are presented in equation and graphical form that are immediately accessible to other workers.

An approach that is not restricted by the limit state conditions was then outlined. This consisted of adapting an existing non-linear solution to incorporate moisture transport and moisture dependent material properties. This can be used to give the adhesive stress and strain distribution throughout the joint for any given loading condition.

Due to the wide range of joint configurations and the non-linear and moisture-dependent material models this is probably the most advanced closed form solution available for adhesively bonded joints.

This approach currently only incorporates the degradation of the cohesive adhesive properties and, thus, is really applicable to those joints where the degraded adhesive forms the weak link. The degradation of the interface between the adhesive and the substrate can be incorporated indirectly by a reduction in the adjacent adhesive material properties. However, in principle it is possible to incorporate the interface directly using fracture mechanics and this is an area for further development. Another area that needs consideration is the effect of swelling strains, due to the absorbed moisture in the adhesive, on the stress distribution within the joint. It should be relatively straightforward to include this effect in the closed form analysis.

ACKNOWLEDGMENTS

The author would like to thank Mr. Stephen Lilley who helped code the moisture dependent analyses.

REFERENCES

[1] Watts, J. F. and Castle, J. E., *J. Mater. Sci.* **19**, 2259–2272 (1984).
[2] Davis, S. J. and Watts, J. F., *J. Mater. Chem.* **6**, 479–493 (1996).
[3] Korenburg, C. F., Kinloch, A. J., and Watts, J. F., *J. Adhesion* **80**, 169–201 (2004).
[4] Parker, B. M., *Vide Les Couches Minces* **50–272**, 590–593 (1994).
[5] Ashcroft, I. A., Digby, R. P., and Shaw, S. J., *J. Adhesion* **75**, 175–202 (2001).
[6] Hamade, R. F. and Dillard, D. A., *J. Adhes. Sci. Tech.* **17–9**, 1235–1264 (2003).
[7] Crocombe, A. D., Hua, Y. X., Loh, W. K., Wahab, M. A., and Ashcroft, I. A., *Int. J. Adhes. Adhes.* **26**, 325–336 (2006).
[8] Liljedahl, C. D. M., Crocombe, A. D., Wahab, M. A., and Ashcroft, I. A., *J. Adhesion Sci. Technol.* **19**, 525–547 (2005).
[9] Volkersen, O., *Luftfahrtforschung* **15**, 41–47 (1938)
[10] Crocombe, A. D., Stress analysis, in *Adhesive Bonding Science Technology and Applications*, R. D. Adams (Ed.) (Woodhead Publishing, Ltd., Cambridge, 2005), Ch. 5, pp. 91–122.
[11] Goland, M. and Reissner, E., *J. Applied Mechanics* **66**, 17–27 (1945).
[12] Volkersen, O., *Construction Metallique* **4**, 3 (1965).
[13] Renton, W. J. and Vinson, J. R., *J. Applied Mechanics* **44**, 101–106 (1977).
[14] Ojalvo, U. and Eidinoff, H. L., *AIAA* **16–3**, 204–211 (1978).
[15] Delale, F., Erdogan, F., and Aydinoglu, M. N., *J. Composite Materials* **15**, 249–271 (1981).
[16] Yang, C. and Pang, S. S., *J. Eng. Matls. and Tech.* **118–2**, 247–255 (1996).
[17] Tsai, M. Y., Oplinger, D. W., and Morton, J., *Int. J. Solids and Structures* **35–12**, 1163–1185 (1998).
[18] Sawa, T. and Suga, H. J., *Adhes. Sci. Tech.* **10–12**, 1255–1271 (1996).
[19] Allman, D. J., *Quart. J. Mech. and Appl. Math.* **30**, 377–386 (1977).
[20] Adams, R. D. and Mallick, V., *J. Adhesion* **38**, 199–217 (1992).
[21] Bogy, D. B., *J. Applied Mechanics*, **35**, 460–466 (1968).
[22] Groth, H. L., *Int. J. Adhes. Adhes.* **8–2**, 107–113 (1988).
[23] Hart-Smith, L. J., NASA Report CR112235, Langley Research Center (1973).
[24] Hart-Smith, L. J., NASA Report CR112236, Langley Research Center (1973).
[25] Bigwood, D. A. and Crocombe, A. D., *Intl. J. Adhes. Adhes.* **9**, 229–242 (1989).
[26] Bigwood, D. A. and Crocombe, A. D., *Int. J. Adhes. Adhes.* **10–1**, 31–41 (1990).
[27] Crocombe, A. D. and Bigwood, D. A., *J. Strain Anal. for Mech. Des.* **27–4**, 211–218 (1992).
[28] Weitsman, Y., *J. Comp. Mat.* **11**, 378–394 (1977).
[29] Crocombe, A. D., *Int. J. Adhes. Adhes.* **9–3**, 145–153 (1989).
[30] Crank, J., *The Mathematics of Diffusion* (Oxford Science Publications, Oxford, 1979), 2nd ed.
[31] Hambly, H. O., "*The strength of adhesive bonded joints degraded by moisture*," Ph.D. Thesis, University of Surrey, Guildford, Surrey, UK (1998).
[32] Loh, W. K., "*Modelling interfacial degradation in adhesively bonded structures*," Ph.D. Thesis, University of Surrey, Guildford, Surrey, UK (2002).
[33] Liljedahl, C. D. M., "*Modelling the interfacial degradation in adhesively bonded joints,*" Ph.D. Thesis, University of Surrey, Guildford, Surrey, UK (2006).
[34] Crocombe, A. D., *Int. J. Adhes. Adhes.* **17–3**, 229–238 (1997).